12th International Kimberlite Conference Extended Abstract No. 12IKC-153, 2024

Experimental investigation of silica enrichment in Archean cratonic lithosphere

Melai, C.[1]; Withers, A.C[2]; Frost, D.[2]and Tomlinson, E. L.[1]
[1]Geology, School of Natural Sciences, Trinity College Dublin, melaic@tcd.ie
[2]Bayerisches Geoinstitute, Universität Bayreuth, tony.withers@uni-bayreuth.de
[1]Geology, School of Natural Sciences, Trinity College, tomlinse@tcd.ie

Introduction

A key challenge in understanding the Archean cratonic lithosphere is the anomalous silica enrichment observed in mantle peridotites. This enrichment cannot be explained by conventional melting models (Herzberg 2004, Walter 1998), prompting investigation into alternative mechanisms. Theoretically, the Si-enrichment can be explained through the interaction between a mantle peridotite and an Al-depleted komatiitic melt (ADK) generated during high pressure melting with garnet in the residue. The komatiitic melt, characterized by low Al_2O_3 content, emerges as a promising candidate due to its minimal influence on both garnet formation and Mg/(Mg+Fe) ratio of the residual peridotite (Aulbach et al. 2011, Tomlinson and Kamber 2021). In the present study, an experimental approach has been undertaken to test this hypothesis. High-pressure experiments were performed to: (i) better understand the incongruent orthopyroxene forming reaction in non-pyrolytic compositions, (ii) provide insight into the effect of komatiite-peridotite reaction on mineral and melt compositions, and (iii) provide insight into the kinetics of the komatiite-peridotite reaction and the relative importance of diffuse porous and channelised melt flow during komatiite transport.

Methods

Synthetic starting materials were prepared as a mixture of pure reagent oxides to recreate three different bulk compositions: (i) fertile peridotite based on natural KR4003 (Mg# 89.3) (Walter 1998), (ii) depleted peridotite (Mg# 89.1), and (iii) Al-poor komatiite (Mg# 84.7). The oxide powders were weighted by stoichiometry and mixed for ~1hr in ethanol in an agate mortar to ensure homogenization. The peridotite powders were pressed into a pellet and decarbonated at 1000°C overnight and reduced in a gas mixing furnace for 24 hrs (T= 1300°C and DFMQ -2 obtained with a gas mixture of CO_2:CO= 60:40). The komatiite powder was instead poured into a Pt crucible and molten at 1650°C for 30 min, then quenched in ice cold water. The final glass was then ground to a homogenous powder in an agate mortar.

The high-pressure multi-anvil experiments were performed at the Bayerisches Geoinstitute in a 1200-tonne Sumitomo press with a 6-8 Kawai-type split-sphere guide blocks system. Two separate sets of experiments

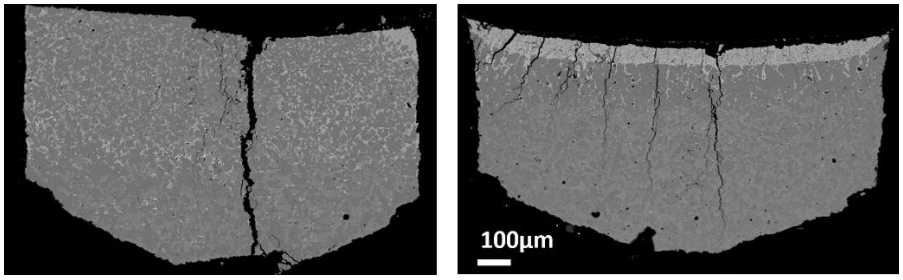

Figure 1: Backscattered SEM images of samples recovered from 1600°C and 5GPa. On the left, sample S8025_D and on the right sample S8025_F.

were conducted: (i) hybrid experiment and (ii) reaction couple experiments. For the hybrid experiments (S8025_F and S8025_D) the powdered fertile (F) and depleted (D) peridotites were loaded in a graphite capsule in a 50%-50% ratio with the komatiite powder and ran for 5hrs at 5 GPa and 1600°C. The recovered samples are shown in figure 1. For the reaction couple experiments (S8030_F), peridotite rods were pre-synthesised at 5 GPa and 1600°C (Fig.2) for both fertile and depleted compositions. The rods were then cut and polished to the correct size and subsequently loaded in a new run with komatiite powder loaded at the bottom of the capsule. The reaction experiment was run for 5hrs at 5 GPa and 1650°C. The successful recovered sample (S8030_F) is shown in figure 3.

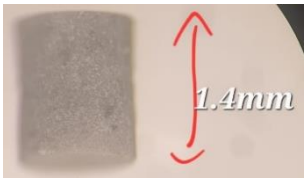

Figure 2: Recovered fertile peridotite rod from a 12 hrs experimental run at 5 GPa 1600°C. A slice of the peridotite cylinder was removed at the top and bottom to ensure the correct length for the next experiment, as well as to check its homogeneity.

Preliminary results

1) *Hybrid experiment* - both experiments reached only low degrees of melting (Tab. 1) and are orthopyroxene-free, containing only olivine + clinopyroxene + garnet in the solid phase assemblage. This indicates that the temperature was below that of the orthopyroxene forming peritectic reaction ol+cpx = opx+melt (Walter 1998). However, the abundance of clinopyroxene in the residue is higher than during melting of peridotite alone at the same melt fraction (Walter 1998), consistent with the thermodynamic modelling results (Tomlinson and Kamber 2021). The higher abundance of clinopyroxene suggests that, once the reaction temperature is reached, the orthopyroxene-forming reaction will be more productive in the hybrid peridotite-komatiite system than it is in the peridotite-only system We expect to see orthopyroxene in future experiments at higher temperature (~1630°C). In the hybrid experiment with depleted peridotite composition, the Mg# in the bulk residue is higher than in the fertile experiment (respectively Mg# 90.3 vs 88.7), while the modal phase relations show lower clinopyroxene and higher olivine. The presence of higher melt % in the depleted run (16% vs 6%) might be due to a temperature gradient in the two-capsule experimental setup.

2) *Reaction couple experiment* - Given the variation in phase abundance along the capsule length (Fig. 3), fertile peridotite-komatiite sample S8030_F was divided in 3 zones: (1) the bottom, the melt zone, (2) the reaction zone; and (3) unreacted peridotite. The mineral assemblage at the boundary (zone 1) is olivine +

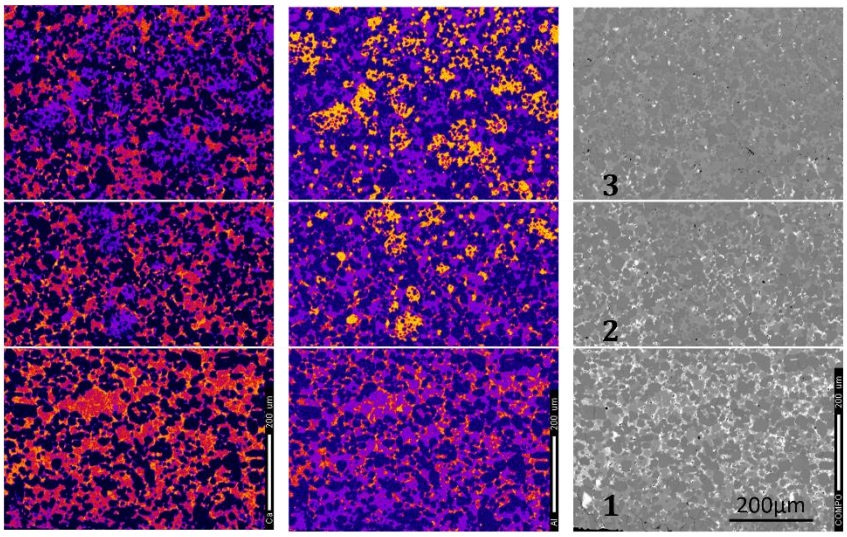

Figure 3: Backscattered SEM image of sample S8030_F (right) together with and Al concentration map in the center to highlight the presence of the garnets, and to the left the Ca map, to highlight the melt.

clinopyroxene suggesting precipitation from the komatiite melt. Further up the capsule (zones 2 + 3), garnet is observed together with olivine and clinopyroxene (Fig. 3). Zone 2 contains melt and has less clinopyroxene in the mineral assemblage than the melt-free zone 3, this suggests that peridotite underwent melting in the zone adjacent to komatiite. However, the abundance of clinopyroxene and absence of orthopyroxene in the peridotite portion of the cell indicates that the peridotite did not melt significantly and the orthopyroxene-forming peritectic reaction was not reached at the temperatures of this experiment. The MgO content of the olivine varies from Fo# 89.7 when in equilibrium with the melt (zone 1) down to Fo# 88.4 in the unreacted zone (zone 3) (Table 1).

The observed abundance of olivine in the melt zone and its high Mg# suggests that olivine may be fractionating from the komatiite melt, which will have the effect of increasing the SiO_2/MgO ratio of the residual melt, increasing its ability to act as an agent of silica enrichment. The potential for fractionation and reaction of komatiite during transport also has implications for the composition of komatiite melts erupted at the surface.

Table 1: Major element phase composition (EMPA) in oxide wt%. Calculated bulk residual after the melting were obtained via mass balance.

sample	setup	phase	SiO_2	TiO_2	Al_2O_3	Cr_2O_3	FeO	MnO	MgO	CaO	Na_2O	Sum	%
S8025_D	hybrid	ol	40.29		0.19	0.14	9.14	0.15	49.02	0.29		99.22	57
		cpx	53.99		4.10	0.52	5.05	0.15	25.94	8.69	0.35	98.79	21
		grt	41.68	0.11	23.24	2.13	5.93	0.22	22.48	4.17		99.96	7
		melt	48.16	0.35	11.15	0.54	7.62	0.22	15.99	13.82	0.68	98.53	16
		bulk res.	44.07	0.01	3.05	0.40	7.93	0.16	41.50	2.68	0.09	99.90	
S8025_F	hybrid	ol	39.92		0.23	0.13	10.16	0.15	47.99	0.30		98.88	51
		cpx	53.53		3.95	0.49	5.60	0.15	24.80	9.68	0.42	98.62	31
		grt	42.04	0.21	22.34	1.75	6.95	0.24	21.39	4.94		99.86	12
		melt	45.96	0.97	10.39	0.42	9.66	0.22	14.19	14.14	0.80	96.75	6
		bulk res.	45.34	0.03	4.25	0.46	8.37	0.16	37.55	4.04	0.14	100.35	
S8030_F 1	react. couple	ol	40.63	0.01	0.20	0.16	9.65	0.15	49.67	0.32	0.02	100.81	56
		cpx	54.06	0.05	4.86	0.63	5.14	0.17	25.65	9.35	0.41	100.32	25
		melt	46.77	0.69	12.15	0.49	8.91	0.23	13.93	14.58	0.76	98.54	19
		bulk res.	44.71	0.02	1.64	0.31	8.24	0.15	42.19	3.10	0.14	100.51	
S8030_F 2		ol	40.53	0.01	0.17	0.14	10.00	0.15	49.34	0.32	0.02	100.69	53
		cpx	53.88	0.09	4.87	0.52	5.18	0.16	24.80	10.16	0.45	100.10	32
		grt	42.32	0.22	22.35	2.00	5.76	0.21	22.24	5.50	0.01	100.60	11
		melt	46.77	0.69	12.15	0.49	8.91	0.23	13.93	14.58	0.76	98.54	4
		bulk res.	45.16	0.06	4.22	0.48	7.89	0.16	38.00	4.20	0.16	100.34	
S8030_F 3		ol	40.41	0.02	0.35	0.13	10.68	0.16	48.69	0.39	0.02	100.85	54
		cpx	53.17	0.11	5.50	0.54	5.09	0.16	23.63	11.32	0.49	100.02	35
		grt	42.29	0.27	22.42	1.92	5.75	0.20	22.13	5.52	0.01	100.52	11
		bulk res.	45.16	0.08	4.62	0.47	8.18	0.16	37.00	4.80	0.18	100.67	

References

Aulbach, S., Stachel, T., Heaman, L.M. et al. (2011) Formation of cratonic subcontinental lithospheric mantle and complementary komatiite from hybrid plume sources. Contrib Mineral Petrol 161, 947–960

Herzberg C. (2004) Geodynamic information in peridotite petrology. J. Petrol. 45, 2507–2530

Tomlinson EL, Kamber, B (2021) Depth-dependent peridotite-melt interaction and the origin of variable silica in the cratonic mantle. Nat. Commun. 12, 1082

Walter MJ (1998) Melting of garnet peridotite and the origin of komatiite and depleted lithosphere. J Petrol 39:29–60.